Neuroscience 277 (2014) 72–86

MLC901, A TRADITIONAL CHINESE MEDICINE INDUCES NEUROPROTECTIVE AND NEUROREGENERATIVE BENEFITS AFTER TRAUMATIC BRAIN INJURY IN RATS

H. QUINTARD, [a,b] **T. LORIVEL,** [a] **C. GANDIN,** [a] **M. LAZDUNSKI** [a] **AND C. HEURTEAUX** [a]*

[a] *Institut de Pharmacologie Moléculaire et Cellulaire, Centre National de la Recherche Scientifique (CNRS), Université Nice Sophia Antipolis, 660 Route des Lucioles, 06560 Valbonne, France*

[b] *Centre Hospitalo-Universitaire de Nice, Hôpital St Roch, 4 rue Pierre Dévoluy, 06000 Nice, France*

Abstract—Traumatic brain injury (TBI) is a frequent and clinically highly heterogeneous neurological disorder with large socioeconomic consequences. NeuroAid (MLC601 and MLC901), a Traditional Medicine used in China for patients after stroke has been previously reported to induce neuroprotection and neuroplasticity. This study was designed to evaluate the neuroprotective and neuroregenerative effects of MLC901 in a rat model of TBI. TBI was induced by a moderate lateral fluid percussion applied to the right parietal cortex. MLC901 was injected intraperitoneally at 2 h post-TBI, and then administered in drinking water at a concentration of 10 mg/ml until sacrifice of the animals. The cognitive deficits induced by TBI were followed by using the ''what-where-when'' task, which allows the measurement of episodic-like memory. MLC901 treatment decreased brain lesions induced by TBI. It prevented the serum increase of S-100 beta (S100B) and neuron-specific enolase (NSE), which may be markers to predict the neurologic outcome in human patients with TBI. MLC901 reduced the infarct volume when injected up to 2 h post-TBI, prevented edema formation and assisted its resolution, probably *via* the regulation of aquaporin 4. These positive MLC901 effects were associated with an upregulation of vascular endothelial growth factor (VEGF) as well as an increase of endogenous hippocampal neurogenesis and gliogenesis around the lesion. Furthermore, MLC901 reduced cognitive deficits induced by TBI. Rats subjected to TBI displayed a suppression of temporal order memory, which was restored by MLC901. This work provides evidence that MLC901 has neuroprotective and neurorestorative actions, which lead to an improvement in the recovery of cognitive functions in a model of traumatic brain injury.

Key words: NeuroAid, traumatic brain injury, neurogenesis, cognitive deficits, aquaporins, VEGF.

INTRODUCTION

Traumatic brain injury (TBI) is the leading cause of mortality in the active/working population and a major cause of disability in people under the age of 35 in Europe and in the USA. With its socioeconomic consequences and its high frequency in young adults, TBI remains a major health problem worldwide and is considered as a real challenge to public health (Bruns and Hauser, 2003; Maas et al., 2008). Despite recent advances in intensive care, the long-term disabilities secondary to brain injury, are still dramatic. 60% of patients still display important after-effects, particularly in cognitive tasks (Ruttan et al., 2008). The complex physiopathology of brain injury after trauma can explain the difficulty to improve prognosis. TBI causes structural damage and functional deficits that are due to both primary and secondary injury mechanisms. Following the initial mechanical insult leading to mechanical disruption of brain tissue, secondary pathways are activated over minutes to months after injury (Andriessen et al., 2010).

Despite a number of neuroprotective therapeutic trials, no broadly applicable, safe and efficacious treatment for TBI has yet been identified (Xiong et al., 2009). NeuroAid (MLC601/MLC901), a Traditional Chinese Medicine (TCM) could represent a new approach as therapeutic strategy against TBI. There are clinical assays, including large-scale clinical trials on the use of this treatment for stroke patients. Several molecular and cellular demonstrations that this combination (mostly herb extracts) targets important pathways of neuroprotection and neurorepair have also been reported (Heurteaux et al., 2013). Limited clinical studies on non-acute stroke patients showed MLC601 improved recovery in terms of functional outcome and neurological disability with a good safety profile (Gan et al., 2008; Siow, 2008; Bittner et al., 2009; Chen et al., 2009; Kong et al., 2009; Young et al., 2010; Bavarsad Shahripour et al., 2011; Harandi et al., 2011; Navarro et al., 2013; Siddiqui

*Corresponding author. Tel: +33-4-93-95-77-84; fax: +33-4-93-95-77-04.
E-mail address: heurteau@ipmc.cnrs.fr (C. Heurteaux).

Abbreviations: AQP, aquaporin; AQP4, aquaporin 4; BDNF, brain-derived neurotrophic factor; BrdU, 5-bromo-2′-deoxyuridine; BWC, brain water content; CHIMES, CHInese Medicine NeuroAid Efficacy on Stroke recovery; DCX, doublecortin; GFAP, glial fibrillary acidic protein; LEP, lateral fluid percussion; MAP2, microtubule-associated protein 2; NeuN, neuron-specific nuclear protein; NSE, Neuron-Specific Enolase; SGZ, subgranular cell layer; S100B, S-100 beta; TBI, traumatic brain injury; TCM, Traditional Chinese Medicine; TTC, 2.3.5-triphenyltetrazolium chloride.

http://dx.doi.org/10.1016/j.neuroscience.2014.06.047
0306-4522/

et al., 2013). In the post hoc analysis of the CHIMES (for CHInese Medicine NeuroAid Efficacy on Stroke recovery) study, which represents the first large clinical trial of high scale (more than 1000 patients) on a TCM in Neurology (Venketasubramanian et al., 2009; Chen et al., 2013a), MLC601 did not clearly demonstrate improvement of the primary outcome but a reduction of early recurrent vascular events and vascular deaths in post-stroke patients has been reported (Chen et al., 2013b). In addition, a recent analysis on more than 500 patients within the CHIMES cohort with more prognostic factors for poorer outcome indicates a positive effect of MLC601 (Navarro et al., 2014). Interestingly, an Australian New Zealand clinical trial including 140 patients with mild or moderate traumatic brain injury and treated with NeuroAid supplementation has been registered in 2013, proving the interest of neurologists for this new potential strategy against TBI (https://www.anzctr.org.au/Trial/Registration/TrialReview.aspx?id=364449).

Consistent with observations of MLC601 efficiency in humans, pharmacological data obtained in rodents have established that MLC601 and MLC901 prevent death of threatened neuronal tissues, decrease cognitive deficits and improve functional outcome by restoring neuronal circuits in models of focal and global ischemia (Heurteaux et al., 2010; Quintard et al., 2011). The efficacy of MLC601/MLC901 has also been demonstrated *in vitro* in a model of excitotoxicity (Heurteaux et al., 2010) and in a model of oxygen glucose deprivation (OGD), which mimics ischemic conditions (Moha Ou Maati et al., 2012). These interesting results led us to evaluate the therapeutic effectiveness of MLC901 in lateral fluid percussion (LFP)-induced TBI in rats. The present work describes the protective/restorative effects of MLC901 against brain damage induced by TBI.

EXPERIMENTAL PROCEDURES

Animals and ethical approval

All experiments were performed on male Sprague–Dawley rats (300 g) from Janvier Laboratories (Saint-Quentin Fallavier, France) and used according to policies on the care and use of laboratory animals of European Communities Council Directive (2010/63/EU). The French ministry of higher education and scientific research approved the experiments (protocol number 00735-02). All efforts were made to minimize animal suffering and reduce the number of animals used.

LFP-induced brain injury

TBI of moderate severity was induced by LFP (Thompson et al., 2005). In brief, rats were anesthetized by inhalation of 2% isoflurane. Core temperature was monitored with a rectal probe and body temperature was maintained at 37 °C with a heating blanket during surgery. Animals were placed in a Kopf stereotaxic frame. The scalp was incised on the midline, and a 3-mm craniotomy was made lateral to the right temporoparietal cortex (coordinates: −3.0 mm anterior posterior and +3.5 mm mediolateral to bregma) with a dental drill, taking care to leave the dura mater intact. A female Luer-Lok fitting was placed over the dura mater, fixed securely into the craniotomy site with dental cement, and then used to attach the rat to the FP injury device. Lateral FP brain injury was induced using a device consisting of a Plexiglas, cylindrical, saline-filled reservoir bound at one end by a Plexiglas plunger mounted on O-rings. The opposite end of the cylinder was capped with a male Luer stub, which was connected to the rat *via* the female Luer-Lok fitting. A pendulum was allowed to drop, striking the plunger and producing a calibrated outflow pressure pulse of 2.2 atmospheres and of 20 ms in duration *via* the rapid injection of saline into the closed cranial cavity. The applied cortical pressure was measured extracranially by a pressure transducer connected to an oscilloscope. Immediately after fluid percussion, the scalp was sutured under anesthesia, and the rats returned to their home cage under temperature and light-controlled conditions. Negative controls were sham-operated rats. Each animal underwent the same surgery except for percussion.

Experimental design

Following TBI rats were randomly divided into three groups: (i) sham-operated rats, (ii) vehicle-treated rats, (iii) MLC901-treated rats. A supplementary sham-operated group treated with MLC901 was used in the behavioral experiments. MLC901 (Moleac, Singapore) combines nine herbal components with the following composition per capsule (Heurteaux et al., 2010): 0.57 g Radix astragali, 0.114 g Radix salvia miltiorrhizae, 0.114 g Radix paeoniae rubra, 0.114 g Rhizoma chuanxiong, 0.114 g Radix angelicae sinensis, 0.114 g *Carthamus tinctorius*, 0.114 g *Prunus persica*, 0.114 g Radix polygalae, 0.114 g Rhizoma acori tatarinowii. MLC901 was diluted in saline (as vehicle) at the concentration of 75 mg/ml (stock solution) and incubated under agitation for 1 h at 37 °C. The solution was then filtered with a 0.22-μm filter. For the time window of protection, rats were intraperitoneally injected with a single dose of MLC901 at a concentration of 0.075 mg/ml (in a bolus of 500 μl) 1, 2 or 3 h after TBI followed by an oral administration in drinking water (10 mg/ml) until the sacrifice of animals. The dose of MLC901 used was selected based on our previous studies, where the injection of 0.075 mg/ml of MLC901 in a bolus of 500 μl induced the best protection against global ischemia (Heurteaux et al., 2010; Quintard et al., 2011). Once the time window of protection was determined (from 1 to 2 h post-TBI, see Fig. 2D), MLC901 was injected within this time window of protection in all the following experiments. Following our previous data on cerebral ischemia (Quintard et al., 2011) and in relation to its previously observed potential regenerative properties (Heurteaux et al., 2010; Quintard et al., 2011), MLC901 was then given in drinking water (10 mg/ml) until the sacrifice of rats at 7, 21 days or 10 weeks post-TBI. The flowchart illustrating the experimental design is given in Fig. 1. The researchers, who carried out the TBI surgery and the measures of brain injury were blinded in regard to the treatment code.

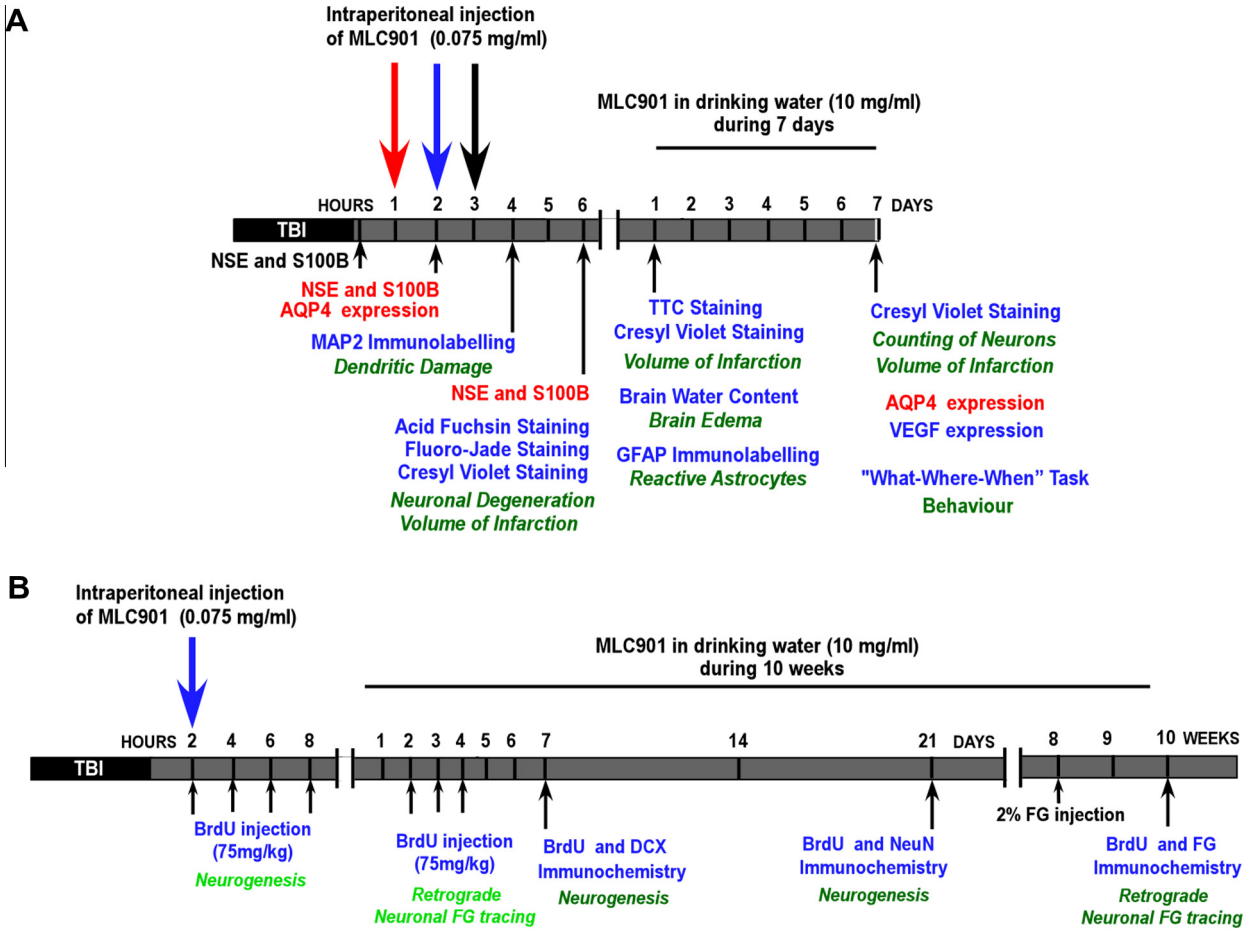

Fig. 1. Flowchart illustrating the different *in vivo* paradigms. In A and B, rats were subjected to lateral fluid percussion (TBI). (A) – MLC901 was administered by intraperitoneal injection (0.075 mg/ml) at 1, 2 or 3 h post-TBI for the determination of the time window of protection. For the other experiments, MLC 901 was injected at 1 or 2 h post-TBI and then administered during 7 days in the drinking water (10 mg/ml). In *red* and *blue* is indicated the technical approach used with the corresponding MLC901 treatment (arrow in red or blue) and in *green* the type of experiment. (B) – MLC901 (0.075 mg/ml) was injected at 2 h post-TBI and then administered in the drinking water (10 mg/ml) during 7 or 21 days for the determination of neurogenesis and during 10 weeks for the retrograde neuronal fluorogold (FG) tracing. In *blue* is indicated the technical approach used with the corresponding MLC901 treatment (arrow blue) and in *green* the type of experiment. For the neurogenesis study, rats received the day of TBI 4 BrdU intraperitoneal injections (75 mg/kg) at 2-h intervals. For the retrograde neuronal FG study, rats were once injected with BRDU (75 mg/kg) at 2, 3 and 4 days post-TBI and received a 2% FG injection 8 weeks after TBI.

Analysis of neurodegeneration by 2.3.5-triphenyltetra zolium chloride (TTC), acid fuchsin and Fluoro-Jade B stainings

The visualization of the lesion extent was firstly obtained from TTC staining as previously described (Heurteaux et al., 2006). The density of injured neurons, *i.e.* the number of injured cells per mm^2 of injured tissue was quantified. A mean value for each brain area was obtained from 10 measurements/section on two sections per slide and 10 slides per rat, for the six animals in each experimental group. Neuronal density values are expressed as mean ± S.D. Fluoro-Jade B staining, which labels degenerative neurons was performed according to the protocol described by Schmued et al. (1997).

Lesion volume analysis on Cresyl Violet stained sections

Every 10th coronal brain section (20 μm) throughout the brain was stained with Cresyl Violet. Photomicrographs were captured using an Olympus microscope and lesion area was determined by using the Olympus® Image software. The Cavalieri formula was used to calculate total lesion volume [Volume = $\Sigma S \times t \times$ ISF] where S = sum of the corrected lesion area surfaces (mm^2), t = section thickness (20 μm) and ISF = inverse of the sampling fraction (1 in 10 sections was counted, *i.e.* sampling fraction 1/10) (n = 6 for each experimental group).

Brain edema

Cerebral edema was determined at 24 h post-TBI by measuring brain water content (BWC) using the wet weight–dry technique (Chen et al., 2008).

Serum quantitation of biochemical markers of traumatic brain injury in the blood: S-100 beta (S100B) and neuron-specific enolase (NSE) measurements

Serum samples were collected on "Vacuette" Z serum Sep clot activator at 10 min, 2, 6 and 24 h after

TBI. S100B and NSE measurements were performed using the Diasorin Liaison XL chemiluminescence immunoassay (Bloomfield et al., 2007).

Immunohistochemistry and Western blotting

Coronal brain sections (40-μm thick) were cut on a vibratome (Leica) and conserved at −20 °C in "antifreeze" medium as previously described (Heurteaux et al., 2010). The antibodies used were the rabbit polyclonal Aquaporin 4 (AQP4) (Antibodies Online, Atlanta, USA, ABIN4984643, diluted 1/300), microtubule-associated protein 2 (MAP2) (1:200, Chemicon International, Merck-Millipore, Saint-Quentin, France) or glial fibrillary acidic protein (GFAP) (1:300, SC6170, Santa Cruz, CliniSciences, Nanterre, France) antibodies. For quantification of protein abundance in the brain tissue, Western blot analysis was performed as previously described (Heurteaux et al., 2010). The blotted membrane was incubated with the following rabbit or goat polyclonal primary antibodies: AQP4 (Antibodies Online, Atlanta, USA, ABIN4984643, diluted 1/300) or vascular endothelial growth factor (VEGF) (1/500, Santa Cruz, CliniSciences, Nanterre, France, SC-1836). Analysis of the fluorescence intensity was performed by using the NIH Image J software (http://rsbwebnih.gov/ij), which allowed to extract the fluorescent intensity levels of cells of each fluorescent image saved as a 16-bit TIFF file ($n = 3$ cultures, 12 wells per experimental group, total 15 fields per condition). Results are given as ratio of mean fluorescence intensity in AU (arbitrary unit)/number of labeled cells ± SEM of three experiments.

Analysis of *in vivo* neurogenesis on brain sections

5-bromo-2′-deoxyuridine (BrdU) treatment consisted of 4 injections (75 mg/kg, *i.p.* each, 2 h interval) the day of the injury. Brains were removed at 24 h after the last BrdU injection. Every sixth section (40 μm) cut throughout the hippocampus was processed for immunohistochemistry using a monoclonal mouse anti-BrdU (1/200; BD Biosciences, Le Pont de Claix, France) (Heurteaux et al., 2010). The phenotype of BrdU-positive cells was determined using fluorescent double-labeling with the following antibodies and dilutions: sheep anti-BrdU (1:200, Interchim, Montluçon, France), goat anti-DCX (doublecortin, 1/200, Santa Cruz Laboratories, CliniSciences, Nanterre, France), mouse anti-NeuN (neuron-specific nuclear protein, 1/250, Millipore, Molsheim, France), rabbit anti-GFAP (glial fibrillary acidic protein, 1/250, Dako, Les Ulis, France) and secondary antibodies conjugated with Alexa Fluor 488 or 594 (1/1000; Molecular Probes, Life Technologies SAS, Saint-Aubin, France).

Neuronal tracer injection

At day 2, 3 and 4 post-TBI, rats were injected with BrdU. Eight weeks after TBI, rats received a bilateral stereotaxic injection of FluoroGold (Fluorochrome INC., Denver, USA), a retrograde neuronal tracer (Sun et al., 2007). The coordinates for the CA3 injection were from bregma: anterior–posterior, −3.3 mm; medial–lateral, 3.2 mm, and the depth from the pial surface, −3.4 mm. Two weeks after FG injection, rats were transcardially perfused with 4% paraformaldehyde and processed for immunohistochemistry as described above.

Behavior: the "what-where-when" task

Seven days (D + 7) after TBI, rats were tested for cognitive deficits using a modified version of object recognition task called the "what-where-when" test. The animals were still being treated with MLC901 during the period of behavioral testing. This test allows to investigate all the aspects of episodic-like memory in rodents (Dere et al., 2005; Barbosa et al., 2010). The test comprises three object exploration trials, designed to simultaneously subsume (i) the memory for location in which objects were explored ("what-where"), and (ii) the temporal order memory for objects presented at distinct time points ("what-when"). The device was an open field made of painted wood, 75 cm square by height 30 cm, and indirectly lit by two halogen lamps (50 lx illumination). Geometric cues were arranged in a spatial frame around the apparatus. Two sets of 4 objects differing in terms of height, color and shape were used. At D + 7 after TBI each rat received two sample trials and a test trial (7 min). In *the first Sample trial* (*Sample 1*), rats were placed in the open-field to explore freely the four copies of a same object (Fig. 6A). After a delay of 90 min, rats received *a second Sample trial* (*Sample 2*) by replacing the 4 objects by 4 novel objects, arranged in a different spatial configuration. After a delay of 180 min, rats received *a test trial* identical to the second sample trial, except that 2 objects from *Sample 1 trial* ("old" objects) and 2 objects known from *Sample 2 trial* ("recent" objects) were present. Furthermore, one of the two "old" objects was shifted to a novel location, whereas both the "recent" objects were presented at identical locations (Fig. 6A).

The behavior of rats was analyzed by ANY-maze tracking software (Anymaze, Stoelting, Wood Dale, USA). The time spent exploring each object was scored and the total exploratory activity was then calculated (sum of the exploration time for each object). We expressed the spatial memory index ("*what-where*" memory) as the preference for the "displaced" old object compared to the "stationary" old object calculated with the following formula:(time spent exploring the "displaced" old object – time spent exploring the "stationary" old object)/time spent exploring both "old" objects". The old objects preference index reflecting the temporal order memory ("*what-when*" memory) was calculated as follows:(time spent exploring both old objects – time spent exploring both recent objects)/total exploration time. Results analysis was restricted to the first 6.5 min of the trials in order to minimize the impact of the object preference erosion naturally occurring with time. The time spent by the rats in the central area of the apparatus (45 cm square) was measured to serve as index of anxiety.

For statistical analysis, the data distribution normality and homoscedasticity were checked using Shapiro–Wilk test for normality and Levene's test for equality of error

variances, respectively. Assumptions for two-way (surgery × treatment) analysis of variance (ANOVA) were never fulfilled. As a consequence, paired and unpaired comparisons were achieved by performing Wilcoxon and Mann–Whitney tests, respectively. In order to verify rats discriminated the stationary ''old'' object (when compared to the displaced ''old'' one) and both ''old'' objects (when compared to ''recent'' ones) above chance level, we used a Mann–Whitney test (with theoretical mean mu = 0). In all cases, statistical significance was accepted as $P < 0.05$.

RESULTS

Neuroprotective effect of MLC901 on the brain damage induced by TBI

As compared to sham-operated uninjured rats, animals subjected to TBI presented neuronal lesions, which were most severe in brain regions surrounding the impact site. Representative photographs of brain slices stained with TTC at the level of the cerebral cortex are shown at 24 h following TBI in Fig. 2A. As indicated by the reduction of the white area on TTC-stained brain slices, cortical infarcts in rats treated with MCL901, administered 2 h after TBI, were strongly reduced. The beneficial effect of MLC901 was confirmed by the quantitative assessment of total lesion volume on Cresyl Violet-stained brain sections at different times following TBI. At 6 h post-TBI, the brain lesion reached a volume of 92.5 ± 10.3 mm^3 that was significantly reduced to 64.5 ± 7 mm^3 by the MLC901-treatment ($P < 0.05$ versus vehicle group) (Fig. 2B). This treatment provided a long-lasting protective effect since the decrease of the lesion volume by MLC901 was sustained at 7 days post-TBI (−43% reduction). The acid fuchsin staining allows to identify injured neurons and follows the specific temporal and regional neuronal injury associated to TBI. At 6 h following TBI the progressive increase in the number of injured neurons in the ipsilateral hippocampal CA3 substructure, dentate gyrus and thalamus of vehicle-treated rats was significantly reduced by MLC901 (Fig 2C, upper panel). Representative photomicrographs of the hippocampal CA3 region on acid fuchsin or Fluoro-Jade B-stained brain sections highlighted the neuronal degeneration induced by TBI and the potent protective effect of MLC901 treatment 6 h after TBI (Fig. 2C, upper panel). Injured neurons stained by acid fuchsin appeared small and round and were surrounded by vacuoles. As compared to vehicle-treated rats, the number of acid fuchsin-positive neurons was strongly decreased in the CA3 area of MLC901-treated rats. (Fig. 2C, bottom panel). Fluoro-Jade B staining, in which degenerative neurons appeared in green, demonstrated a strong neuronal degeneration in vehicle-treated rats (Fig. 2C, upper panel, right side). TBI-induced necrotic and apoptotic neuronal death was significantly reduced after a MLC901-treatment (Fig. 2C). The MLC901 time window of protection was determined by *i.p.* injection of 0.075 mg/ml (in a bolus of 500 µl) 1, 2 or 3 h post-TBI followed by an oral administration of MLC901 in drinking water at the concentration of 10 mg/ml until sacrifice at 7 days (Fig. 2D). The MLC901 treatment provided a significant protection when the first injection was within 2 h following TBI. When treatment was delayed to 3 h after TBI, the number of surviving cortical neurons was comparable to that observed in vehicle-treated rats ($P > 0.05$), suggesting that the capacity to protect was lost after 3 h following TBI.

Effect of MLC901 on reactive astrocytes and dendritic damage

GFAP is the cell-specific intermediate filament in astrocytes and the upregulation of its synthesis is considered a definite feature of activated astrocytes (Kernie et al., 2001). Clearly, a positive GFAP staining was observed both in the injured cortex and dentate gyrus of vehicle-treated rats but not of the sham-operated animals at 24 h following TBI. MLC901 strongly decreased GFAP expression in both injured structures (Fig. 3A, B). A quantitative analysis (Fig. 3C, D) showed that GFAP expression was respectively increased 1.80 and 3.0-fold in the cortex and the dentate gyrus of vehicle-treated rats as compared to the sham group ($^{**}P < 0.01$). A MLC901 treatment allowed to return to sham levels of GFAP expression in both cerebral structures.

The MAP2 is abundantly expressed in the soma and dendrites of neuronal cells. MAP2 is important for microtubule stability and neural plasticity. Alterations in MAP2 expression are of key importance in neuronal degeneration following brain injury (Johnson and Jope, 1992). At 4 h following TBI, we observed a strong decrease of MAP2 expression in the CA3 region as well as in the dentate gyrus of injured vehicle-treated rats. This MAP2 alteration was prevented in MLC901-treated rats (Fig. 3B–E). The quantitative analysis of MAP2 expression in the dentate gyrus and the hippocampal CA3 substructure confirmed the result (Fig. 3D–F). In the CA3 of vehicle-treated rats, the levels of MAP2 expression were significantly 1.48-fold decreased as compared to sham rats, whereas in the MLC901-treted animals they were comparable to those observed in the sham group ($^{**}P < 0.01$). This result suggests that MLC901 reduces dendritic damage in the spared neurons after TBI.

Effect of MLC901 on serum protein biomarkers, S100B and NSE

Then, we analyzed the concentration of two predictive serum markers, S100B and NSE, used for trying to predict the neurologic outcome in human patients with TBI (Kovesdi et al., 2010; Giacoppo et al., 2012). Significant increases in serum S100B and NSE levels were detected up to 6 h post-TBI in vehicle-treated rats as compared to sham-operated animals ($^{*}P < 0.05$ versus sham group; Fig. 4). A peak was observed for both proteins at 2 h following TBI. Very interestingly, MLC901, which was injected 1 h post-TBI strongly prevented this serum increase of both S100B and NSE ($^{\#}P < 0.05$ versus vehicle-treated TBI group; Fig. 4).

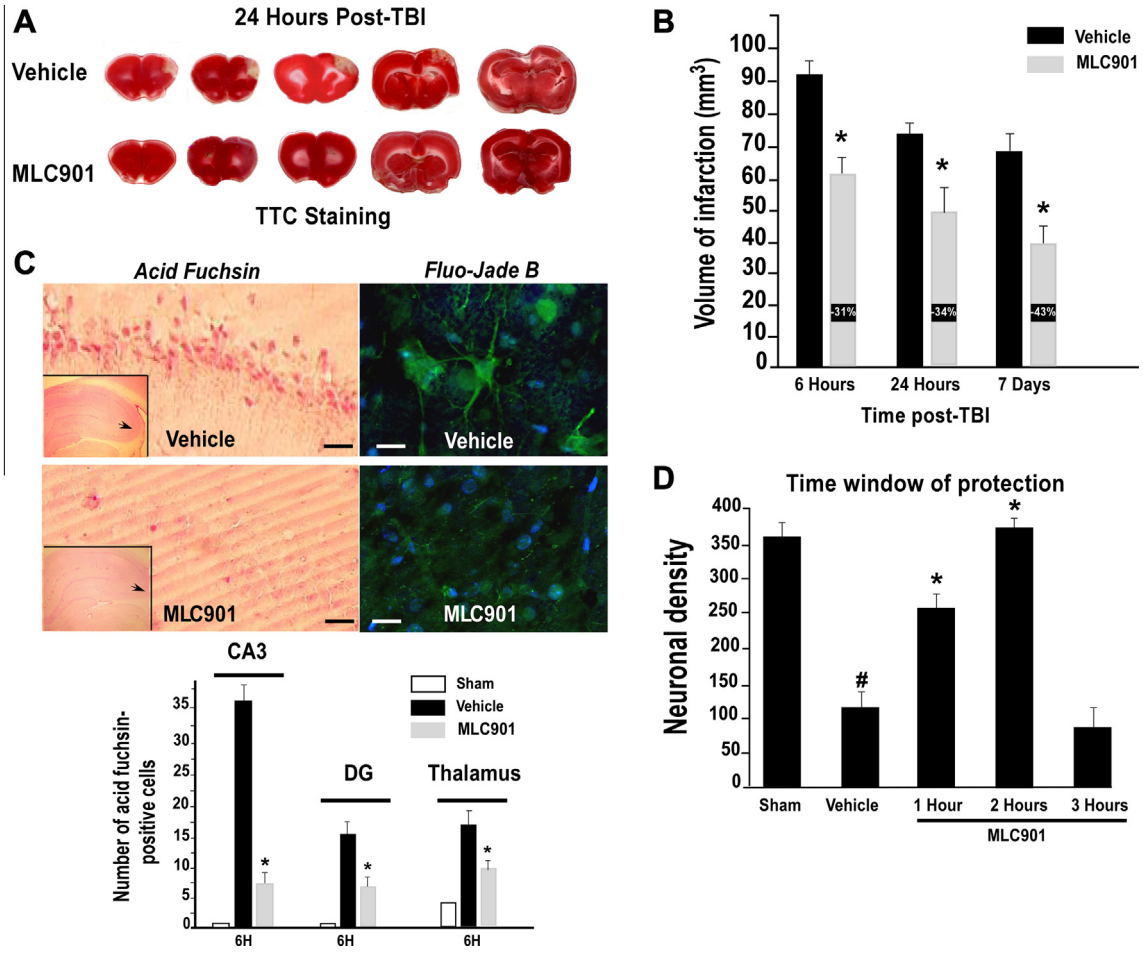

Fig. 2. Neuroprotective effects of MLC901 in rats subjected to TBI, highlighting by TTC, Acid Fuchsin, Fluoro-Jade and Cresyl Violet stainings. (A) – Representative photographs of coronal TTC-stained brain sections 24 h after TBI. MLC901 was *i.p.* injected 2 h after TBI at a concentration of 0.075 mg/ml (500 µl/rat). (B) – Volume of cortical damage (mm^3) at different times after TBI assessed by Cresyl Violet staining. Animals received an *i.p.* MLC901 injection (0.075 mg/ml in a bolus of 500 µl) 2 h post-TBI followed by an oral administration in drinking water (10 mg/ml) for 7 days. Rats were sacrificed at 6, 24 h or 7 days post-TBI. (C) *Upper panel* – Representative photographs of Acid Fuchsin- (left side) or Fluoro-Jade (right side)-stained hippocampal brain sections 6 h after TBI. Scale bars = 25 and 10 µm, respectively. (C) *Bottom panel* – Number of acid fuchsin-positive cells per mm^2 in CA3, dentate gyrus and thalamus at 6 h after TBI (n = 6 rats per experimental group). (D) – Time window of protection of a MLC treatment (0.075 mg/ml) on the neuronal density per mm^2 7 days after TBI. (n = 6 per experimental group, $^{*}P < 0.05$ versus vehicle TBI group, $^{\#}P < 0.05$ versus sham group). Data are mean ± SEM assessed by ANOVA and post hoc Tukey's w test. (n = 6 per experimental group). Values in columns represent the percentage of reduction in lesion volume.

Effect of MLC901 on cerebral edema formation and aquaporin expression

Cerebral edema was determined by measuring BWC in cortical segments. Edema formation was evaluated at 24 h post-injury. As previously observed (Shenaq et al., 2012; Khaksari et al., 2013; Du et al., 2013), BWC in sham-operated rats was around 71%. TBI led to an increase of the BWC, demonstrating a brain edema within the ipsilateral injured hemisphere (77.3 ± 0.5%) (Fig. 5A). BWC was significantly reduced by the MLC901-treatment administered 2 h after TBI (71.9 ± 0.5%, $^{*}P < 0.05$).

Aquaporins (AQPs), and in particular AQP4, the most abundant AQP in the brain, have dual roles in the formation and then the resolution of edema after brain injury (Badaut et al., 2011). Early inhibition of the water channels has positive effects in the prevention of edema formation. However, at a later time point, during the course of brain injury (few days), AQP4 is important for the clearance of water from the brain to the blood vessels (Fukuda and Badaut, 2012). Using Western blotting assay, AQP4 protein expression was found to be significantly reduced (−20%) in the ipsilateral cortex of vehicle-treated group as compared to sham-operated animals 2 h following TBI ($P < 0.05$) (Fig. 5B). This decrease of AQP4 expression was more pronounced in rats treated with MLC901 1 h post-TBI (−40%). In contrast, 7 days following TBI, we observed a strong increase of AQP4 expression in MLC901-treated group as compared to vehicle-treated rats (Fig. 5B). Two hours following TBI, the high AQP4 immunolabeling was diffusely distributed within the contusional cortex of vehicle-treated rats, and was strongly decreased in the MLC901-treated animals (Fig. 5C, upper panel). In contrast, at 7 days post-TBI, MLC901 induced an increase in AQP4 expression, which was mainly located at the periphery of blood vessels (Fig. 5C, bottom panel).

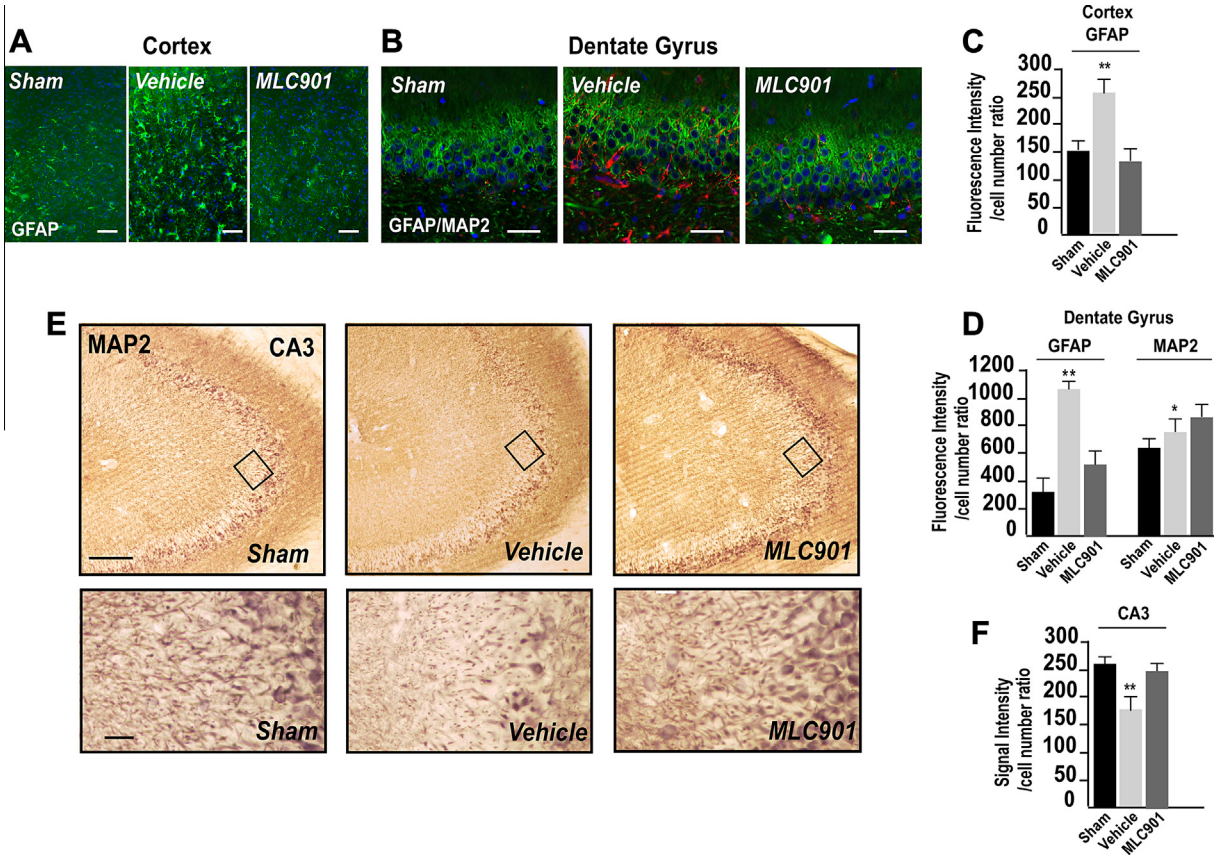

Fig. 3. MLC901 prevents the upregulation of GFAP and the alteration of MAP2 expression induced by TBI. (A) – GFAP immunolabeling (green) in a portion of the ipsilateral cortex adjacent to the lesion observed in sham-operated, TBI-vehicle- or MLC901-treated rats at 24 days following TBI (Scale bar = 15 μm). (B) – Double-labeling of GFAP (red) and MAP2 (green) in dentate gyrus from 3 experimental groups (Scale bar = 20 μm). (C and D) – Quantification of GFAP and MAP2 signal intensity in immunostained neurons of the cortex and dentate gyrus. Data are expressed as ratio of mean fluorescence intensity in AU (arbitrary unit × 1000) to number of labeled cells ± SEM. Average fluorescence intensity was expressed from two independent experiments (n = 8 sections per experimental group, 15 fields per section and analyzed in triplicate) ($^{**}P < 0.01$, $^{*}P < 0.05$ versus sham and MLC901 groups). (E) – MAP2 peroxidase-immunostaining in hippocampal CA3 region from 3 experimental groups 4 h post-TBI. Scale Bar = 50 μm. Bottom panels – High-magnification photomicrographs of the boxed area in upper panels showing in more detail the pattern of MAP2 immunolabeling. Scale Bar = 10 μm. Animals received an *i.p.* MLC901 injection (0.075 mg/ml in a bolus of 500 μl) 2 h post-TBI. (F) – Quantification of MAP2 signal intensity in immunostained neurons of CA3 substructure. Data are expressed as ratio of mean signal intensity in AU (arbitrary unit x1000) to number of labeled cells ± SEM as described above. ($^{**}P < 0.01$ versus sham and MLC901 groups).

Stimulation of the neurotrophic factor expression VEGF by MLC901 after TBI

The release and up-regulation of endogenous neurotrophic factors such as BDNF (brain-derived neurotrophic factor) and VEGF is an important mechanism in neuronal repair after brain damage (Ferrara, 2004). MLC901 is known to stimulate BDNF expression in brain tissue after focal and global ischemia (Heurteaux et al., 2010; Quintard et al., 2011). In this work, we evaluated 7 days after TBI changes in VEGF expression in the ipsilateral cortex and hippocampus of vehicle- and MLC901-treated rats by using Western blot assays. VEGF levels significantly increased in hippocampus and not in the cortex of vehicle-treated rats at 7 days post-TBI (Fig. 5D, $^{*}P < 0.05$). MLC901 significantly stimulated VEGF expression both in hippocampus and cortex of animals as compared to the vehicle-treated group ($^{\#}P < 0.05$).

Post-TBI stimulation of hippocampal neurogenesis and gliogenesis around the lesion by MLC901

Traumatic injury stimulates neurogenesis in the dentate subgranular cell layer (SGZ) (Nakatomi et al., 2002). However brain self-repair by spontaneous neurogenesis is not sufficient to induce an extensive recovery. To test the MLC901 potential in enhancing hippocampal neurogenesis, the incorporation of BrdU (5-bromo-2′-deoxyuridine, a DNA synthesis marker) in dividing progenitor cells, corresponding to the production of newborn neurons was analyzed 7 and 21 days after TBI. One week after TBI, the number of BrdU-positive cells increased three-fold in the ipsilateral hippocampus of the TBI vehicle-group, compared to that observed in the sham-operated group (Fig. 6A, $^{*}P < 0.05$). MLC901 increased 2.6-fold the number of BrdU-positive cells in the DG as compared to the vehicle-treated group 7 days after TBI ($^{\#}P < 0.05$) (Fig. 6A). The phenotype of BrdU-positive

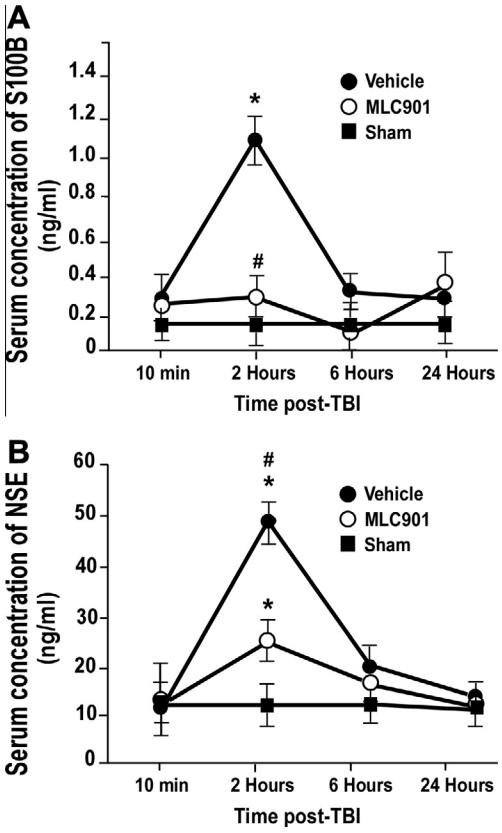

Fig. 4. Effect of MLC901 on the serum concentrations of S100B and NSE (ng/ml), used as biomarkers at different times after TBI. Rats received an *i.p.* MLC901 injection 1 h following TBI. Data are mean ± SEM ($n = 6$ per experimental group, $^{*}P < 0.05$ versus sham operated group, $^{\#}P < 0.05$ versus vehicle TBI group).

cells in the SGZ was analyzed by double-labeling with DCX, a microtubule-associated protein that is specifically expressed in migrating neuronal precursors and in areas of continuous neurogenesis in the adult brain for neurons. Many of the DCX-labeled cells were closely associated with BrdU in DG (Fig. 6B). BrdU + cells did not co-localize with GFAP. Twenty-one days after TBI, the number of BrdU-positive cells in MLC901-treated injured group was still significantly increased as compared to that observed in the vehicle-treated injured group ($^{\#}P < 0.05$, Fig. 6A–C). At day 21 post-TBI, fluorescent double labeling for BrdU and NeuN (a mature neuron marker) was performed to follow the differentiation of the new proliferating cells. MLC901 significantly increased the percentage of BrdU/NeuN co-labeled cells in the DG (59.8% in MLC901 group versus 18.4% in the vehicle group). At 21 days following TBI, we also observed an increase in the number of BrdU-positive cells in the area surrounding the injured cortex of vehicle-treated rats as compared to the sham-operated group. Interestingly, MLC901 strongly increased the BrdU labeling in the same injured area (Fig. 6D). BrdU-positive cells co-localized with GFAP suggesting that these newly generated cells within the entire region around the injured site had matured to fully differentiated astrocytes. These results are in favor of a regenerative potential of MLC901 to replenish the population of damaged and/or destroyed cells.

To analyze whether new mature granule neurons generated following TBI can establish the correct anatomical connection to the existing hippocampal circuitry, rats were intraperitoneally injected with BrdU at Day 2, 3 and 4 post-TBI, followed 8 weeks later by the injection of the retrograde neuronal tracer FG into the granule cell target structure, CA3 (Sun et al., 2007). Animals were allowed to survive 2 additional weeks to provide sufficient time for retrograde transportation of FG from the CA3 to the DG granular layer. Using a confocal microscope, we observed that the hippocampal FG injection induced an intense labeling of the neuronal cell bodies in the granule cell layer, which retrogradely incorporated the fluorescent dye (Fig. 6F) in all experimental groups. Then, to determine whether the newly generated cells retrogradely labeled with FG, we observed BrdU + cells which were colocalized with FG in the dentate gyrus of both injured vehicle- and MLC901-treated rats (Fig. 6G). It then appeared that MLC901 increased the number of BrdU/FG double-labeled cells, indicating that MLC901, which stimulates hippocampal neurogenesis also increases the number of axons of newly generated cells to the CA3 region (Fig. 6G).

Improvement in cognitive function recovery by MLC901

TBI induces reproducible cognitive deficits which can be measured by using the ''what, where, when'' task (Fig. 7A). To ensure that anxiety is not involved in the behavior of rats in this task, we measured the time spent in the center of the open field (a classical index of anxiety). The results showed that this time duration was dependent neither on the treatment received (Vehicle vs MLC901) nor on the fact that animals were exposed to lateral percussion (Sham vs TBI) (Fig. 7B). Thus, the anxiety level of animals in our conditions is unlikely to account for the differences of object preference observed between groups. In Fig. 7C, we observed that both TBI groups, with or without MLC901 treatment, significantly displayed decreased exploratory activity toward all objects (= total exploratory activity) when compared to respective sham groups during samples trials (Fig. 7C; $U = 15$, $^{**}P < 0.01$ for Vehicle-TBI rats). This drop of exploration capacity was also observed in the test trial, but only significant in the MLC901-TBI group (Fig. 7C; $^{*}P < 0.05$). All rats spent less time exploring the objects during the test trials than during the sample trials, probably due to habituation to the experimental environment. This difference was significant for the four groups (Fig. 7C; Vehicle-Sham: $T = 8$; $^{\$}P < 0.05$/MLC901-Sham: $T = 0$; $^{\$\$}P < 0.01$/Vehicle-TBI: $T = 2$; $^{\$\$}P < 0.01$/MLC901-TBI: $T = 1$; $^{\$}P < 0.05$). In the analysis of temporal order memory, the two sham groups (vehicle and MLC901) showed a significant preference for the ''old'' objects (Fig. 7D; Vehicle-Sham: $U = 55$; $^{\#\#}P < 0.01$/MLC901-Sham: $U = 65$; $^{\#\#}P < 0.01$). There was no significant difference (Fig. 7D; $U = 35$; $P > 0.05$), when we compared the Vehicle-Sham rats to MLC901-Sham rats, suggesting an absence of drug effect on sham animals in the temporal task. TBI totally abolished the

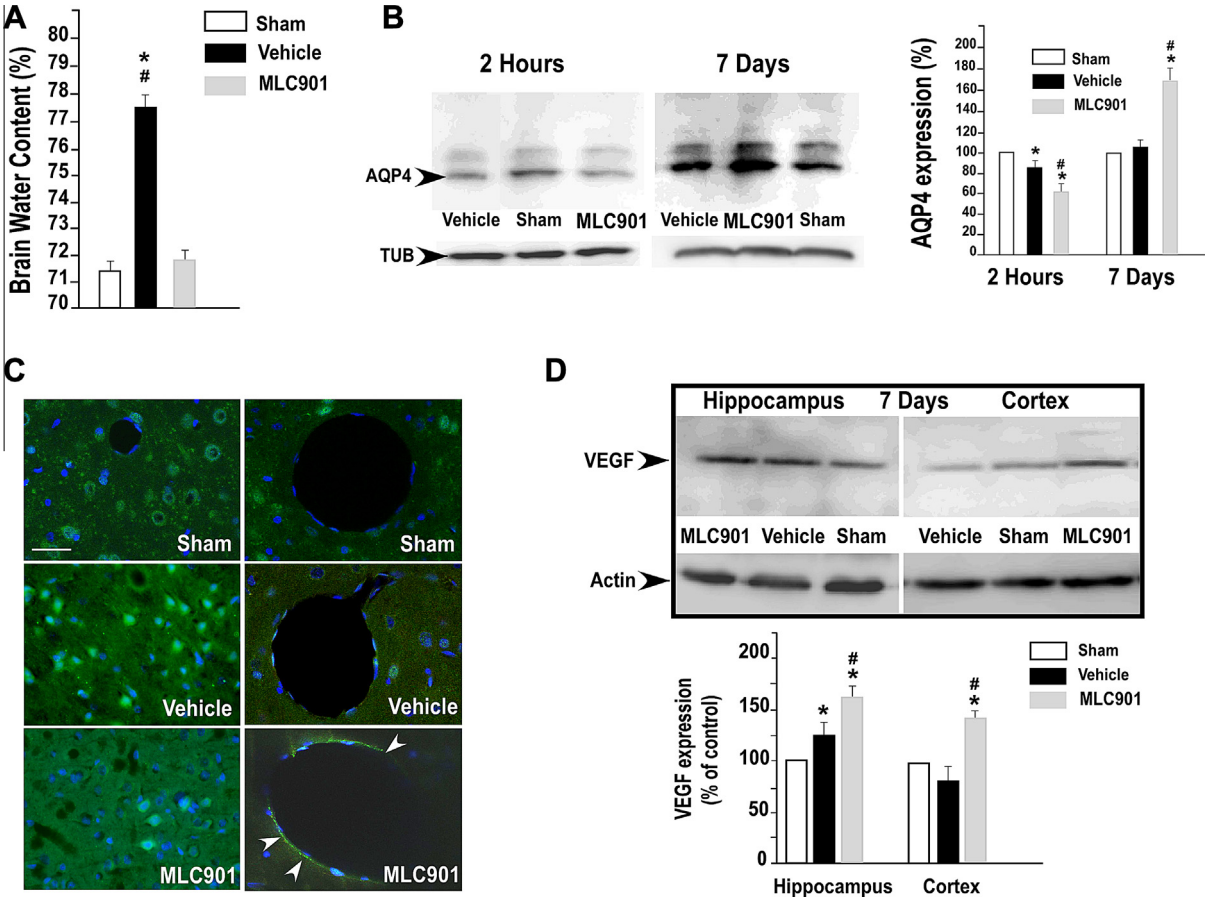

Fig. 5. Effect of MLC901 on cerebral edema formation, AQP4 and VEGF expression in rats subjected to a lateral fluid percussion-induced TBI. (A) – Brain water content 24 h post-TBI. It was measured in ipsilateral contusional cortical segments and presented as percentage of water content. Data are mean ± SEM (n = 6 per experimental group, $^{*}P < 0.05$ versus sham operated group and $^{\#}P < 0.05$ versus vehicle TBI group). Rats received an *i.p.* MLC901 injection 2 h following TBI. (B) – AQP4 expression (30 kDa) in injured cortical tissue determined by Western blotting analysis at 2 h and 7 days post-TBI. Tubulin was used as internal control for the loading of protein level. *Left panel*: Western blot, *Right panel*: Quantitation of AQP4 expression obtained in Western blots in the 3 experimental groups. Values are expressed as a percentage of control. Data are mean ± SEM ($^{*}P < 0.05$ versus sham operated group and $^{\#}P < 0.05$ versus vehicle TBI group). (C) – Representative photomicrographs of the MLC901-induced decrease of AQP4 immunolabeling (in green) in the ipsilateral injured cortex at 24 h post-TBI (*Left panel*) and the MLC901-induced increase of AQP4 immunolabeling at the periphery of blood vessels at 7 days post-TBI (*Right panel*). (D) Western blotting analysis of brain VEGF expression (*Upper panel*) and its quantitation (*Bottom panel*) in the hippocampal and cortical samples from sham-operated, TBI vehicle- or MLC901-treated rats at 7 days post-TBI. The band of VEGF was observed at 42 kDa in the whole-cell fraction from rat brains. Actin was used as internal control. Histograms represent relative VEGF expression obtained in Western blotting in the 3 experimental groups. Values are expressed as a percentage of control. Data are mean ± SEM assessed by ANOVA and post hoc Tukey's w test, $^{*}P < 0.05$ versus sham-operated group, $^{\#}P < 0.05$ versus vehicle TBI group. MLC901 was *i.p* injected 2 h after TBI followed by an oral administration in drinking water (10 mg/ml) during 7 days after traumatic injury. Western blots data are representative of 3 separate experiments (n = 6 per group).

preference for ''old'' objects. TBI rats treated with vehicle failed to discriminate between the two ''old'' objects and the two ''recent'' ones. They did not perform above chance level (Fig. 7D; $U = 42.5$; $P > 0.05$). Very interestingly, MLC901 completely reversed this severe impairment and restored the performance of the MLC901-treated TBI rats to that observed in sham rats (Fig. 7D; $U = 42$; $^{\#}P < 0.05$). The MLC901-TBI rats performances were above chance level and similar to those of MLC901-Sham rats. In addition, the old objects preference index was significantly higher in the MLC901-TBI rats than in the Vehicle-TBI rats ($^{\S}P < 0.05$). These results showed that MLC901 allows the recovery of the temporal order memory, which is impaired after TBI. In term of object location (spatial) memory (old ''stationary'' object versus old ''displaced'' object), vehicle-treated rats, with or without TBI, did not show preference for any of the ''old'' objects. They did not significantly perform above chance level (Fig. 7D Inset; Vehicle-Sham: $U = 21$; $P > 0.05$/Vehicle-TBI: $U = 45$; $P > 0.05$). There was no significant difference between the Vehicle-Sham and Vehicle-TBI groups for the spatial preference index (Fig. 7D Inset; $U = 29$; $P > 0.05$). In contrast, both Sham-rats and TBI-animals treated with MLC901 spatially discriminated between the two ''old'' objects with a similar level of performance. They performed above chance level in exploring the ''displaced'' and the ''stationary'' objects and showed a preference for the ''stationary'' object (Fig. 7D Inset; preference for the ''stationary'' object versus the ''displaced'' object: MLC901-Sham: $U = 48$; $^{\#}P < 0.05$/MLC901-TBI: $U = 42$; $^{\#}P < 0.05$). These results show that MLC901 itself has a positive effect on object location (spatial) memory, which is maintained in TBI-rats.

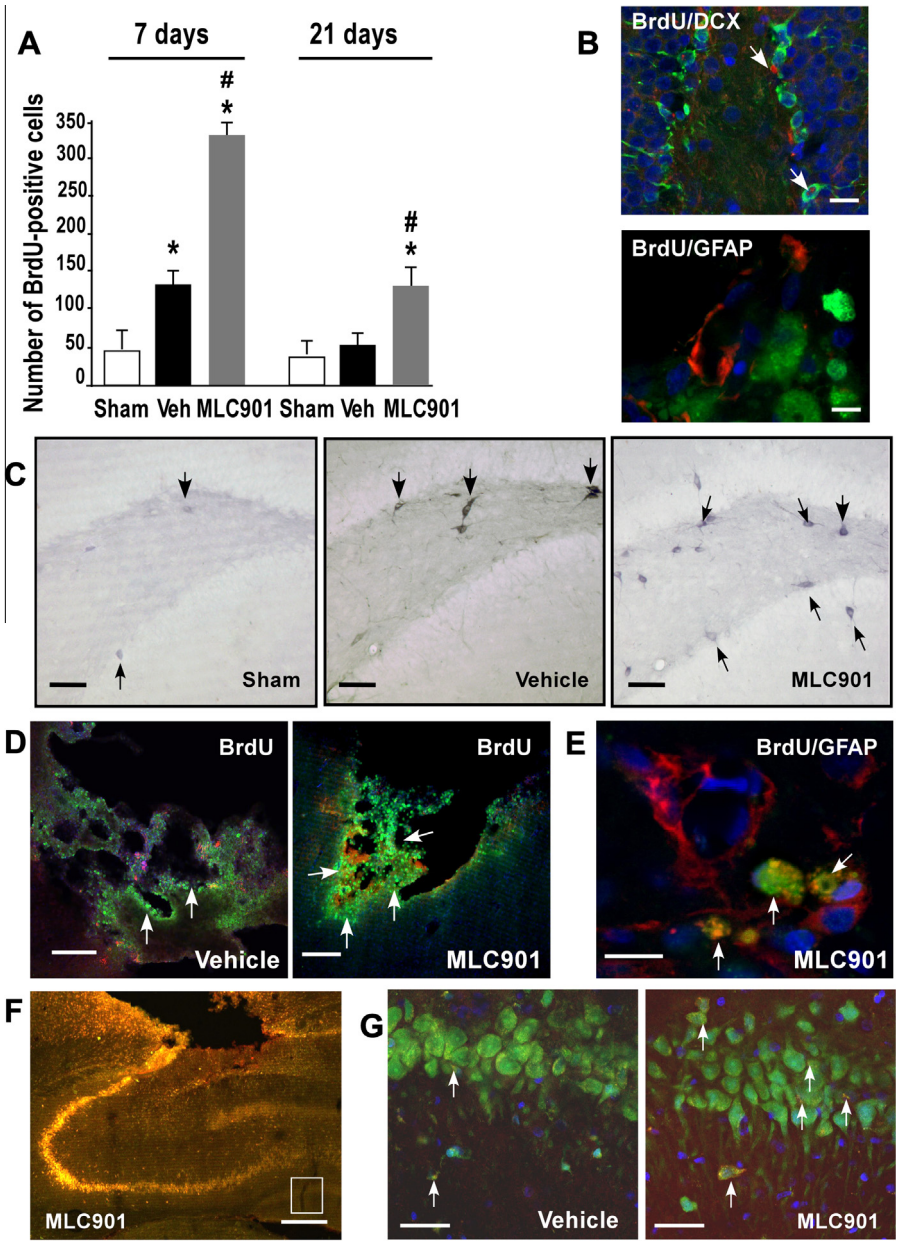

Fig. 6. Stimulating effect of MLC901 on neurogenesis induced by TBI. (A) – Quantitation of BrdU-positive cells per hippocampus from sham-operated, TBI-vehicle- or MLC901-treated rats at 7 and 21 days after TBI. Data are expressed as mean ± SEM (3 independent experiments from $n = 6$ per group, 8 sections per group, 10 fields per section, chosen randomly; $^{*}P < 0.05$ versus sham-operated group, $^{\#}P < 0.05$ versus TBI vehicle-treated rats). (B) – *Upper Panel*: Double-labeling of BrdU-labeled neurons (in green) with DCX neuronal precursor marker (in red) 24 h after TBI. Scale Bar = 5 μm. Arrows indicate the BrdU/DCX co-localization. *Bottom panel*: Double-labeling of BrdU-labeled neurons (in green) with GFAP, an astrocyte marker (in red) 24 h after TBI. (C) – Representative photomicrographs of BrdU peroxidase-staining (arrows) in hippocampal dentate gyrus from the 3 experimental groups 21 days after TBI. Scale Bar = 20 μm. (D) – Intense MLC901-induced increase of BrdU labeling (arrows) in the proximal cortical injury zone 21 days after TBI. Scale Bar = 30 μm. (E) – Double-labeling of BrdU-labeled neurons (in green) with GFAP (in red) 21 days after TBI. Arrows indicate the BrdU/GFAP co-localization. (F) – Hippocampal coronal section of a MLC901-treated TBI rat that had received a FluoroGold (FG) injection in the CA3 region at 8 weeks post-TBI. The neuronal cell bodies in the granule cell layer, which retrogradely incorporated FG, are apparent in the boxed area. Scale Bar = 100 μm. (G) – Confocal micrograph in F showing co-localization (arrows) of BrdU (green) Scale Bar = 5 μm. (red), highlighting the projection of axons of newly generated neurons to the hippocampal CA3 region. Rats were *i.p.* injected with a single dose of MLC901 (0.075 mg/ml in a bolus of 500 μl) 2 h after TBI followed by an oral administration in drinking water (10 mg/ml) until sacrifice.

DISCUSSION

Due to the complexity of TBI, there is increasing evidence that the search for a drug which specifically acts on a single target is exceeded and that combination therapies comprising more than one active ingredient can represent a better strategy. Interestingly, combination therapy has been advocated for centuries by prescriptions of formulae in TCM to treat a wide variety of ailments. TCM, which is based on clinical experience

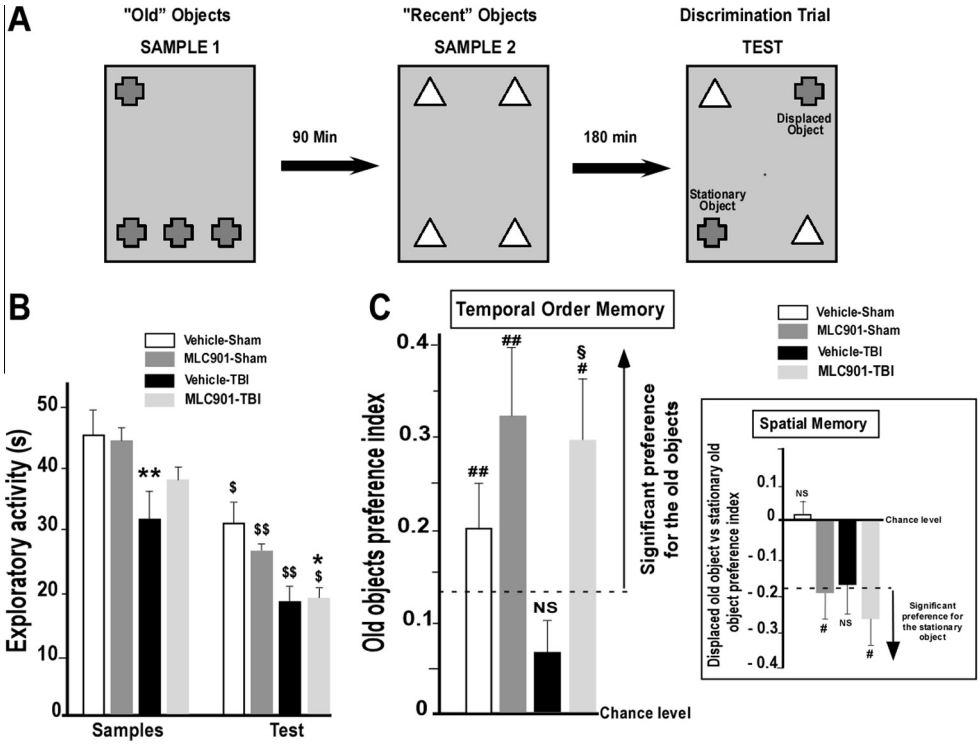

Fig. 7. MLC901 reverses TBI-related impairments of the episodic memory in the ''what, when, where'' task. The experimental groups were as follows: Vehicle-Sham, $n = 10$; MLC901-Sham, $n = 11$; Vehicle-TBI, $n = 10$; MLC901-TBI, $n = 9$. MLC901 (0.075 mg/ml, 500 μl/rat) was *i.p* injected 2 h post-TBI followed by an oral administration in drinking water (10 mg/ml) during 7 days. All values are mean ± SEM. (A) – Schematic drawing of the experimental design used. (B) – Anxiety level of animals. Neither the surgery nor MLC901 modified the anxiety-related behaviors of mice as detected by the time spent in the central area of the open field. All values are mean ± SEM. *Sample 1 trial:* Vehicle-Sham vs MLC901-Sham: $U = 52$; $P > 0.05$/Vehicle-TBI vs MLC901-TBI: $U = 25.5$; $P > 0.05$/Vehicle-Sham vs Vehicle-TBI: $U = 37.5$; $P > 0.05$/MLC901-Sham vs MLC901-TBI: $U = 41$; $P > 0.05$. (C) – Total exploratory activity. Only the first 6.5 minutes of each trial were considered. The samples exploratory time was obtained by averaging the *sample* 1 and *sample* 2 exploratory times. Comparison between Vehicle-Sham and Vehicle-TBI rats during the Samples trials: $U = 15$; $^{**}P < 0.01$. Comparison between Samples and Test exploratory times: Vehicle-Sham: $T = 8$; $^{\$}P < 0.05$/MLC901-Sham: $T = 0$; $^{\$\$}P < 0.01$/Vehicle-TBI: $T = 2$; $^{\$\$}P < 0.01$/MLC901-TBI: $T = 1$; $^{\$}P < 0.05$. (D) – Temporal order memory as denoted by preference index for the ''old'' objects during the first 6.5-min trial test. Comparison to chance level: Vehicle-Sham: $U = 55$; $^{\#\#}P < 0.01$/MLC901-Sham: $U = 65$; $^{\#\#}P < 0.01$/Vehicle-TBI: $U = 42.5$; $^{NS}P > 0.05$/MLC901-TBI: $U = 42$; $^{\#}P < 0.05$. Comparison between Vehicle-TBI and MLC901-TBI: $U = 18$; $^{\S}P < 0.05$. *Inset*: Object location (spatial) memory as denoted by the preference index for the ''stationary'' versus the ''displaced'' old object during the first 6.5-min trial test. Comparison to chance level: Vehicle-Sham: $U = 21$; $^{NS}P > 0.05$/Vehicle-TBI: $U = 45$; > 0.05/MLC901-Sham: $U = 48$; $^{\#}P < 0.05$/MLC901-TBI: $U = 42$; $^{\#}P < 0.05$.

and consists of several types of medicinal herbs or several types of medicinal herb extracts, has now attracted increasing attention both from industry and academia. As recently shown for promyelocytic leukemia, Chinese herbal medicines can now represent a new promising area in drug discovery (Wang et al., 2008). Among all herbal Chinese formulae proposed for cerebrovascular diseases, NeuroAid has recently emerged as a promising treatment against stroke. Several clinical trials and reports have revealed a high level of safety (Gan et al., 2008; Young et al., 2010; Harandi et al., 2011; Siddiqui et al., 2013) as well as efficiency in improving cerebral blood flow velocity and stroke rehabilitation, even at a late stage (Siow, 2008; Gan et al., 2008; Chen et al., 2009; Kong et al., 2009; Venketasubramanian et al., 2009; Bavarsad Shahripour et al., 2011; Navarro et al., 2013). The CHIMES trial (Chen et al., 2013a) has not shown that MLC601 could improve the primary outcome but revealed efficiency of the drug on the early recurrent vascular events in post-stroke patients (Chen et al., 2013b). In addition a further analysis within the CHIMES trial on more than 500 patients with more prognostic factors for poorer outcome indicates a beneficial effect of MLC601 (Navarro et al., 2014). Recent preclinical studies on MLC601/901 provide a solid scientific support to the proposed use of this therapeutic compound against stroke (Heurteaux et al., 2013).

The present study indicates that MLC901 induces a brain protection against the deleterious effects induced by TBI and enhances neurological recovery. The LFP brain injury model used in that work is highly reproducible and a well-characterized model of experimental traumatic brain injury (Dixon et al., 1987). MLC901 strongly ameliorated the histopathological results, highlighted by a decrease of the brain lesion volume. In this model of moderate TBI, the lesions were maximal in the cortical area surrounding the impact site and in the hippocampus, ipsilateral to the impact site. This finding is in accordance with previous observations (McIntosh et al., 1989).

S100B and NSE have been proposed as potential predictive biomarkers of recovery in traumatic brain

injury (Giacoppo et al., 2012). S100B, a calcium-binding protein found in astroglia and Schwann cells, is a marker of brain damage and glial activation. Clinically, several reports have found a correlation between serum S100B level and the outcome of patients (Raabe et al., 1998; Woertgen et al., 1999; Rothermundt et al., 2003). NSE is a cytoplasmic glycolytic enzyme of neurons, which is passively released into the extracellular space, only under pathological conditions. Increased levels of NSE have been found in blood of patients after TBI correlating with clinical outcome (Herrmann et al., 2001; Vos et al., 2004; Berger et al., 2006). However, conflicting results have also been reported showing no difference between control and patients (Ross et al., 1996; Raabe et al., 1998). In the present study, TBI in rats induced increases of both S100B and NSE proteins and MLC901 treatment largely eliminated these TBI-induced variations. This result suggests a positive effect of MLC901 on the outcome in rats after TBI by decreasing the deleterious consequences induced by TBI from severe to moderate or mild.

Another consequence of TBI is the appearance of cerebral edema, which is one of the most critical factors in patient's morbidity and mortality. The degree and extent of edema correlates with a negative clinical outcome (Marmarou et al., 2007). Occurring within the closed confines of the skull and meninges, overall brain swelling leads to life-threatening cessation of the brain blood supply due to raised intracranial pressure and damage to cerebral tissue. In rodents and humans, the development of a massive brain edema after TBI is associated with a biphasic pathophysiological response. First, there is a brief period of increased water diffusion distance caused by the transient opening of the blood–brain barrier, which produces predominantly vasogenic edema formation, immediately after injury. Second, at approximatively 45 min post-injury, a more widespread and slower cellular edema formation, caused by neurotoxic edema and astrocytic swelling is initiated and is sustained one or two weeks after TBI (Barzo et al., 1997; Marmarou et al., 2006). This work shows that edema was significantly reduced after a MLC901 treatment, decreasing the risk of uncontrolled high intracranial pressure. One critical mediator of post-traumatic edema is AQPs, and particularly AQP4 (Fukuda and Badaut, 2012). AQPs are water channels that are involved in the prevention and the resolution of edema (Badaut et al., 2011). Twenty four hours after traumatic brain injury a decrease of AQP4 immunostaining is observed, specifically in regions affected by the BBB break-down, whereas an increase appears on the border of the insult 3 days after injury (Ke et al., 2001). Interestingly, as compared to vehicle, MLC901 induced a significant decrease of AQP4 expression in the first hours after TBI followed by an increase one week later. As already observed after a post-TBI treatment with anti-AQP4 antibodies (Shenaq et al., 2012) the early decrease of AQP4 after brain trauma may be an indication of a protective effect against vasogenic edema formation, whereas the late increase could be essential for long-term cytotoxic edema resolution (Taniguchi et al., 2000; Ke et al., 2001). These data suggest a potential role of MLC901 during edema resolution by acting on AQP4 expression which would be expected to facilitate water extravasations from the brain parenchyma to liquid compartments including blood vessels and CSF.

It is now well accepted that the functional recovery that occurs spontaneously after brain injury (stroke or TBI) is due to the plasticity of surviving neurons, lesion-induced plasticity, and/or plasticity of neural connections (Murphy and Corbett, 2009; Schoch et al., 2012). The proliferation of newly generated cells contributes to the overall cellular remodeling that occurs after TBI (Richardson et al., 2010). We observed that the proximal injury zone is marked largely by newly generated cells. In addition, more distal to the injury area we observed a neurogenesis which occurs within the subgranular zone of the dentate gyrus. The newly generated cells differentiate into mature DG granule cells which form synapses and send axons to their target region CA3, indicating their successful integration into the existing neuronal circuitry. These results suggest that MLC901 treatment stimulates both gliogenesis and neurogenesis, which probably help in inducing a dynamic brain remodeling and lead to a better neurologic recovery in the first weeks after TBI. The positive effects of MLC901 on neuronal plasticity (as characterized by increased neurogenesis, neurite outgrowth, axonal sprouting, dendritic arborization and/or synaptogenesis) has already been observed following focal and global ischemia and correlated to functional recovery (Heurteaux et al., 2010; Quintard et al., 2011). The growth promoting factors such as BDNF and VEGF are key mediators to support adaptive remodeling of surviving neurons and neural networks, which benefits the recovery progress (Conte et al., 2003; Chopp et al., 2009). VEGF is a key mediator of tissue repair after brain injury and is known to play a critical role in angiogenesis (Greenberg and Jin, 2005). An upregulation of BDNF induced by a MLC901 treatment has been previously reported in the context of brain injury caused by stroke and cardiac arrest (Heurteaux et al., 2010; Quintard et al., 2011). In the present work we show that MLC901 increases the expression of VEGF, suggesting that MLC901's effects on this neurotrophic factor could be, at least partially, responsible for benefits observed after this treatment.

It is known that neuronal damage induced by TBI associated to post-traumatic cellular dysfunctions leads to behavioral impairments in rodents, which reflect motor and cognitive deficits observed in humans. Impairments in learning and memory (including impairments in short-term memory, speed of information processing, attention and executive functions) occur in as many as 50% of patients following TBI (McAllister et al., 2006). Similar impairments occur in rodent models (Morales et al., 2005). MLC901 has been previously reported to decrease neurologic deficits and improve recovery after stroke and cardiac arrest in rodents (Heurteaux et al., 2010; Quintard et al., 2011). In the present work we determined the potential effects of MLC901 on TBI-induced episodic memory impairments. Episodic memory is a complex cognitive skill integrating the spatial (''where'') and temporal (''when'') aspects as well as the

object (''what'') of a discrete event (Tulving, 2001). Its disruption commonly observed in traumatic brain-injured patients (Arenth et al., 2012) can be particularly handicapping. In the current study we used a new approach of behavior with a modified version of the novel object recognition task (NORT) which allows to investigate the ''what-where-when'' dimensions of episodic memory in rodents (Dere et al., 2005; Kart-Teke et al., 2006). Consistent with previous data obtained in the classical version of the object recognition task (Davis et al., 2010), this work clearly indicates that TBI rats showed a decrease in object exploration during the sample trials. They also displayed a total suppression of temporal order memory, which had already been observed in cranially injured rats submitted to an olfactory preference task (Gurkoff et al., 2012) and in TBI patients (Schmitter-Edgecombe and Seelye, 2012). While MLC901 failed to reverse the TBI-induced exploratory impairment, it completely restored the temporal order memory demonstrating that its physiological curative/protective effects were translated in behavioral improvement.

The lack of discrimination between both ''displaced'' and ''stationary'' old objects in vehicle-treated sham rats suggests that the spatial characteristics of our task were probably too challenging (visual cues not clear enough, displacement of the displaced object too short...) and exceeded their cognitive capacities. It might be surprising at first sight to observe that the cognitive capabilities of sham rats were different for temporal order memory and object location (spatial) memory. A probable explanation is that the fine neurobiological circuitries underlying the two types of memory are not totally identical. They seem to be processed by different subregions of the hippocampus (Howland et al., 2008). While the ventral hippocampus is crucial for temporal order memory, it is not for the object location (spatial) memory. In the same way, the medial prefrontal cortex is more crucially involved in the temporal order memory than in the object location (spatial) memory (Barker and Warburton, 2011). The segregation of neurobiological substrates for the different types of memory could account, at least in part, for the difference of behavior observed in the present work. In contrast, the capacity of MLC901-treated sham rats, conserved in MLC901-treated TBI rats, to efficiently acquire object location (spatial) memory suggests a pro-cognitive effect of MLC901. This would be consistent with the fact that hippocampal neurogenesis and elevated BDNF secretion are both stimulated by MLC901 (Heurteaux et al., 2010; Quintard et al., 2011) and are known to improve spatial discrimination and consolidation of spatial memory by hippocampus (Garthe et al., 2009; Sahay et al., 2011; Ozawa et al., 2014).

CONCLUSION

This work provides evidence that MLC901 has neuroprotective and neurorestorative actions which lead to an improvement in the recovery of cognitive functions in a rat model of traumatic brain injury and a rationale for exploring MLC901 therapy to improve recovery of patients with TBI.

AUTHOR CONTRIBUTIONS

Conceived and designed the experiments: HQ, CH; Performed the experiments: HQ (surgery), TL (behavior), CG (biochemistry); Analyzed the data: HQ, ML, CH; Wrote the manuscript: ML, CH.

DISCLOSURE/CONFLICT OF INTEREST

This work is supported by a CNRS/MOLEAC contract. ML is vice-president for research of Moleac.

Acknowledgments—The authors are very grateful to D. Picard (Moleac Singapore) for discussions concerning the program and the follow-up of the clinical effects of MLC601 and for providing MLC901 capsules. They are grateful to P. Ferrari for NSE and S100B dosing in the Biochemistry department of the Nice University Hospital (CHU). We are grateful to Dr A. Patel for carefully reading the manuscript. This work is supported by the Centre National de la Recherche Scientifique (CNRS). HQ is very grateful for the financial support of CNRS/CHU Nice.

This paper is dedicated to the memory of Dr M. Vasseur who has been at the origin of the NeuroAid project.

REFERENCES

Andriessen TM, Jacobs B, Vos PE (2010) Clinical characteristics and pathophysiological mechanisms of focal and diffuse traumatic brain injury. J Cell Mol Med 14:2381–2392.

Arenth PM, Russell KC, Scanlon JM, Kessler LJ, Ricker JH (2012) Encoding and recognition after traumatic brain injury: neuropsychological and functional magnetic resonance imaging findings. J Clin Exp Neuropsychol 34:333–344.

Badaut J, Ashwal S, Obenaus A (2011) Aquaporins in cerebrovascular disease: a target for treatment of brain edema? Cerebrovasc Dis 31:521–531.

Barbosa FF, Pontes IM, Ribeiro AM, Silva RH (2010) Extending possible applications of an episodic-like memory task in rats. Behav Brain Res 215:326–331.

Barker GR, Warburton EC (2011) When is the hippocampus involved in recognition memory? J Neurosci 31:10721–10731.

Barzo P, Marmarou A, Fatouros P, Hayasaki K, Corwin F (1997) Contribution of vasogenic and cellular edema to traumatic brain swelling measured by diffusion-weighted imaging. J Neurosurg 87:900–907.

Bavarsad Shahripour R, Shamsaei G, Pakdaman H, Majdinasab N, Nejad EM, Sajedi SA, Norouzi M, Hemmati A, Manouchehri RH, Shiravi A (2011) The effect of NeuroAiD (MLC601) on cerebral blood flow velocity in subjects' post brain infarct in the middle cerebral artery territory. Eur J Intern Med 22:509–513.

Berger RP, Dulani T, Adelson PD, Leventhal JM, Richichi R, Kochanek PM (2006) Identification of inflicted traumatic brain injury in well-appearing infants using serum and cerebrospinal markers: a possible screening tool. Pediatrics 117:325–332.

Bittner S, Meuth SG, Gobel K, Melzer N, Herrmann AM, Simon OJ, Weishaupt A, Budde T, Bayliss DA, Bendszus M, Wiendl H (2009) TASK1 modulates inflammation and neurodegeneration in autoimmune inflammation of the central nervous system. Brain 132:2501–2516.

Bloomfield SM, McKinney J, Smith L, Brisman J (2007) Reliability of S100B in predicting severity of central nervous system injury. Neurocrit Care 6:121–138.

Bruns Jr J, Hauser WA (2003) The epidemiology of traumatic brain injury: a review. Epilepsia 44(Suppl. 10):2–10.

Chen XR, Besson VC, Beziaud T, Plotkine M, Marchand-Leroux C (2008) Combination therapy with fenofibrate, a peroxisome proliferator-activated receptor alpha agonist, and simvastatin, a 3-hydroxy-3-methylglutaryl-coenzyme A reductase inhibitor, on

experimental traumatic brain injury. J Pharmacol Exp Ther 326:966–974.
Chen C, Venketasubramanian N, Gan RN, Lambert C, Picard D, Chan BP, Chan E, Bousser MG, Xuemin S (2009) Danqi Piantang Jiaonang (DJ), a traditional Chinese medicine, in poststroke recovery. Stroke 40:859–863.
Chen CL, Venketasubramanian N, Lee CF, Wong KS, Bousser MG (2013a) Effects of MLC601 on early vascular events in patients after stroke: the CHIMES study. Stroke 44:3580–3583.
Chen CL, Young SH, Gan HH, Singh R, Lao AY, Baroque 2nd AC, Chang HM, Hiyadan JH, Chua CL, Advincula JM, Muengtaweepongsa S, Chan BP, de Silva HA, Towanabut S, Suwanwela NC, Poungvarin N, Chankrachang S, Wong KS, Eow GB, Navarro JC, Venketasubramanian N, Lee CF, Bousser MG (2013b) Chinese medicine Neuroaid efficacy on stroke recovery: a double-blind, placebo-controlled, randomized study. Stroke 44:2093–2100.
Chopp M, Li Y, Zhang ZG (2009) Mechanisms underlying improved recovery of neurological function after stroke in the rodent after treatment with neurorestorative cell-based therapies. Stroke 40:S143–145.
Conte V, Royo C, Shimizu S, Saatman K, Watson D, Graham D, Stocchetti N, McIntosh T (2003) Neurotrophic factors, pathophysiology, and therapeutic applications in traumatic brain injury. Eur J Trauma 29:335–355.
Davis AR, Shear DA, Chen Z, Lu XC, Tortella FC (2010) A comparison of two cognitive test paradigms in a penetrating brain injury model. J Neurosci Methods 189:84–87.
Dere E, Huston JP, De Souza Silva MA (2005) Integrated memory for objects, places, and temporal order: evidence for episodic-like memory in mice. Neurobiol Learn Mem 84:214–221.
Dixon CE, Lyeth BG, Povlishock JT, Findling RL, Hamm RJ, Marmarou A, Young HF, Hayes RL (1987) A fluid percussion model of experimental brain injury in the rat. J Neurosurg 67:110–119.
Du AL, Ji TL, Yang B, Cao JF, Zhang XG, Li Y, Pan S, Zhang B, Hu ZB, Zeng XW (2013) Neuroprotective effect of AG490 in experimental traumatic brain injury of rats. Chin Med J (Engl) 126:2934–2937.
Ferrara N (2004) Vascular endothelial growth factor: basic science and clinical progress. Endocr Rev 25:581–611.
Fukuda AM, Badaut J (2012) Aquaporin 4: a player in cerebral edema and neuroinflammation. J Neuroinflamm 9:279.
Gan R, Lambert C, Lianting J, Chan ES, Venketasubramanian N, Chen C, Chan BP, Samama MM, Bousser MG (2008) Danqi Piantan Jiaonang does not modify hemostasis, hematology, and biochemistry in normal subjects and stroke patients. Cerebrovasc Dis 25:450–456.
Garthe A, Behr J, Kempermann G (2009) Adult-generated hippocampal neurons allow the flexible use of spatially precise learning strategies. PLoS One 4:e5464.
Giacoppo S, Bramanti P, Barresi M, Celi D, Foti Cuzzola V, Palella E, Marino S (2012) Predictive biomarkers of recovery in traumatic brain injury. Neurocrit Care 16:470–477.
Greenberg DA, Jin K (2005) From angiogenesis to neuropathology. Nature 438:954–959.
Gurkoff GG, Gahan JD, Ghiasvand RT, Hunsaker MR, Van K, Feng JF, Shahlaie K, Berman RF, Lyeth BG, Folkerts MM (2012) Evaluation of metric, topological, and temporal ordering memory tasks after lateral fluid percussion injury. J Neurotrauma 30:292–300.
Harandi AA, Abolfazli R, Hatemian A, Ghragozlee K, Ghaffar-Pour M, Karimi M, Shahbegi S, Pakdaman H, Tabasi M, Tabatabae AL, Nourian A (2011) Safety and efficacy of MLC601 in Iranian patients after stroke: a double-blind, placebo-controlled clinical trial. Stroke Res Treat 2011:721613.
Herrmann M, Curio N, Jost S, Grubich C, Ebert AD, Fork ML, Synowitz H (2001) Release of biochemical markers of damage to neuronal and glial brain tissue is associated with short and long term neuropsychological outcome after traumatic brain injury. J Neurol Neurosurg Psychiatry 70:95–100.
Heurteaux C, Laigle C, Blondeau N, Jarretou G, Lazdunski M (2006) Alpha-linolenic acid and riluzole treatment confer cerebral protection and improve survival after focal brain ischemia. Neuroscience 137:241–251.
Heurteaux C, Gandin C, Borsotto M, Widmann C, Brau F, Lhuillier M, Onteniente B, Lazdunski M (2010) Neuroprotective and neuroproliferative activities of NeuroAid (MLC601, MLC901), a Chinese medicine, in vitro and in vivo. Neuropharmacology 58:987–1001.
Heurteaux C, Widmann C, Moha ou Maati H, Quintard H, Gandin C, Borsotto M, Veyssiere J, Onteniente B, Lazdunski M (2013) NeuroAiD: properties for neuroprotection and neurorepair. Cerebrovasc Dis 35(Suppl. 1):1–7.
Howland JG, Harrison RA, Hannesson DK, Phillips AG (2008) Ventral hippocampal involvement in temporal order, but not recognition, memory for spatial information. Hippocampus 18:251–257.
Johnson GV, Jope RS (1992) The role of microtubule-associated protein 2 (MAP-2) in neuronal growth, plasticity, and degeneration. J Neurosci Res 33:505–512.
Kart-Teke E, De Souza Silva MA, Huston JP, Dere E (2006) Wistar rats show episodic-like memory for unique experiences. Neurobiol Learn Mem 85:173–182.
Ke C, Poon WS, Ng HK, Pang JC, Chan Y (2001) Heterogeneous responses of aquaporin-4 in oedema formation in a replicated severe traumatic brain injury model in rats. Neurosci Lett 301:21–24.
Kernie SG, Erwin TM, Parada LF (2001) Brain remodeling due to neuronal and astrocytic proliferation after controlled cortical injury in mice. J Neurosci Res 66:317–326.
Khaksari M, Mahmmodi R, Shahrokhi N, Shabani M, Joukar S, Aqapour M (2013) The effects of Shilajit on brain edema, intracranial pressure and neurologic outcomes following the traumatic brain injury in rat. Iran J Basic Med Sci 16:858–864.
Kong KH, Wee SK, Ng CY, Chua K, Chan KF, Venketasubramanian N, Chen C (2009) A double-blind, placebo-controlled, randomized phase II pilot study to investigate the potential efficacy of the traditional Chinese medicine Neuroaid (MLC 601) in enhancing recovery after stroke (TIERS). Cerebrovasc Dis 28:514–521.
Kovesdi E, Luckl J, Bukovics P, Farkas O, Pal J, Czeiter E, Szellar D, Doczi T, Komoly S, Buki A (2010) Update on protein biomarkers in traumatic brain injury with emphasis on clinical use in adults and pediatrics. Acta Neurochir (Wien) 152:1–17.
Maas AI, Stocchetti N, Bullock R (2008) Moderate and severe traumatic brain injury in adults. Lancet Neurol 7:728–741.
Marmarou A, Signoretti S, Fatouros PP, Portella G, Aygok GA, Bullock MR (2006) Predominance of cellular edema in traumatic brain swelling in patients with severe head injuries. J Neurosurg 104:720–730.
Marmarou A, Lu J, Butcher I, McHugh GS, Murray GD, Steyerberg EW, Mushkudiani NA, Choi S, Maas AI (2007) Prognostic value of the Glasgow Coma Scale and pupil reactivity in traumatic brain injury assessed pre-hospital and on enrollment: an IMPACT analysis. J Neurotrauma 24:270–280.
McAllister TW, Flashman LA, McDonald BC, Saykin AJ (2006) Mechanisms of working memory dysfunction after mild and moderate TBI: evidence from functional MRI and neurogenetics. J Neurotrauma 23:1450–1467.
McIntosh TK, Vink R, Noble L, Yamakami I, Fernyak S, Soares H, Faden AL (1989) Traumatic brain injury in the rat: characterization of a lateral fluid-percussion model. Neuroscience 28:233–244.
Moha Ou, Maati H, Borsotto M, Chatelain F, Widmann C, Lazdunski M, Heurteaux C (2012) Activation of ATP-sensitive potassium channels as an element of the neuroprotective effects of the Traditional Chinese Medicine MLC901 against oxygen glucose deprivation. Neuropharmacology 63:692–700.
Morales DM, Marklund N, Lebold D, Thompson HJ, Pitkanen A, Maxwell WL, Longhi L, Laurer H, Maegele M, Neugebauer E, Graham DI, Stocchetti N, McIntosh TK (2005) Experimental models of traumatic brain injury: do we really need to build a better mousetrap? Neuroscience 136:971–989.

Murphy TH, Corbett D (2009) Plasticity during stroke recovery: from synapse to behaviour. Nat Rev Neurosci 10:861–872.

Nakatomi H, Kuriu T, Okabe S, Yamamoto S, Hatano O, Kawahara N, Tamura A, Kirino T, Nakafuku M (2002) Regeneration of hippocampal pyramidal neurons after ischemic brain injury by recruitment of endogenous neural progenitors. Cell 110:429–441.

Navarro JC, Molina MC, Baroque Ii AC, Lokin JK (2013) The use of NeuroAiD (MLC601) in postischemic stroke patients. Rehabil Res Pract 2012:506387.

Navarro JC, Gan HH, Lao AY, Baroque II AC, Hiyadan JHB, Chua CL, San Jose MCZ, Advincula JM, Lee CF, Bousser MG, Chen CLH (2014) Baseline characteristics and treatment responses of patients included from the Philippines in the CHIMES study. Abstract from session Acute stroke: new treatment concepts. 23th European Stroke Conference Nice.

Ozawa T, Yamada K, Ichitani Y (2014) Hippocampal BDNF treatment facilitates consolidation of spatial memory in spontaneous place recognition in rats. Behav Brain Res 263:210–216.

Quintard H, Borsotto M, Veyssiere J, Gandin C, Labbal F, Widmann C, Lazdunski M, Heurteaux C (2011) MLC901, a traditional Chinese medicine protects the brain against global ischemia. Neuropharmacology 61:622–631.

Raabe A, Grolms C, Keller M, Dohnert J, Sorge O, Seifert V (1998) Correlation of computed tomography findings and serum brain damage markers following severe head injury. Acta Neurochir (Wien) 140:787–791 [discussion 791–782].

Richardson RM, Singh A, Sun D, Fillmore HL, Dietrich 3rd DW, Bullock MR (2010) Stem cell biology in traumatic brain injury: effects of injury and strategies for repair. J Neurosurg 112:1125–1138.

Ross SA, Cunningham RT, Johnston CF, Rowlands BJ (1996) Neuron-specific enolase as an aid to outcome prediction in head injury. Br J Neurosurg 10:471–476.

Rothermundt M, Peters M, Prehn JH, Arolt V (2003) S100B in brain damage and neurodegeneration. Microsc Res Tech 60:614–632.

Ruttan L, Martin K, Liu A, Colella B, Green RE (2008) Long-term cognitive outcome in moderate to severe traumatic brain injury: a meta-analysis examining timed and untimed tests at 1 and 4.5 or more years after injury. Arch Phys Med Rehabil 89:S69–76.

Sahay A, Scobie KN, Hill AS, O'Carroll CM, Kheirbek MA, Burghardt NS, Fenton AA, Dranovsky A, Hen R (2011) Increasing adult hippocampal neurogenesis is sufficient to improve pattern separation. Nature 472:466–470.

Schmitter-Edgecombe M, Seelye AM (2012) Recovery of content and temporal order memory for performed activities following moderate to severe traumatic brain injury. J Clin Exp Neuropsychol 34:256–268.

Schmued LC, Albertson C, Slikker Jr W (1997) Fluoro-Jade: a novel fluorochrome for the sensitive and reliable histochemical localization of neuronal degeneration. Brain Res 751:37–46.

Schoch KM, Madathil SK, Saatman KE (2012) Genetic manipulation of cell death and neuroplasticity pathways in traumatic brain injury. Neurotherapeutics 9:323–337.

Shenaq M, Kassem H, Peng C, Schafer S, Ding JY, Fredrickson V, Guthikonda M, Kreipke CW, Rafols JA, Ding Y (2012) Neuronal damage and functional deficits are ameliorated by inhibition of aquaporin and HIF1alpha after traumatic brain injury (TBI). J Neurol Sci 323:134–140.

Siddiqui FJ, Venketasubramanian N, Chan ES, Chen C (2013) Efficacy and safety of MLC601 (NeuroAiD(R)), a traditional Chinese medicine, in poststroke recovery: a systematic review. Cerebrovasc Dis 35(Suppl. 1):8–17.

Siow CH (2008) Neuroaid in stroke recovery. Eur Neurol 60:264–266.

Sun D, McGinn MJ, Zhou Z, Harvey HB, Bullock MR, Colello RJ (2007) Anatomical integration of newly generated dentate granule neurons following traumatic brain injury in adult rats and its association to cognitive recovery. Exp Neurol 204:264–272.

Taniguchi M, Yamashita T, Kumura E, Tamatani M, Kobayashi A, Yokawa T, Maruno M, Kato A, Ohnishi T, Kohmura E, Tohyama M, Yoshimine T (2000) Induction of aquaporin-4 water channel mRNA after focal cerebral ischemia in rat. Brain Res Mol Brain Res 78:131–137.

Thompson HJ, Lifshitz J, Marklund N, Grady MS, Graham DI, Hovda DA, McIntosh TK (2005) Lateral fluid percussion brain injury: a 15-year review and evaluation. J Neurotrauma 22:42–75.

Tulving E (2001) Episodic memory and common sense: how far apart? Philos Trans R Soc Lond B Biol Sci 356:1505–1515.

Venketasubramanian N, Chen CL, Gan RN, Chan BP, Chang HM, Tan SB, Picard D, Navarro JC, Baroque 2nd AC, Poungvarin N, Donnan GA, Bousser MG (2009) A double-blind, placebo-controlled, randomized, multicenter study to investigate CHInese Medicine Neuroaid Efficacy on Stroke recovery (CHIMES Study). Int J Stroke 4:54–60.

Vos PE, Lamers KJ, Hendriks JC, van Haaren M, Beems T, Zimmerman C, van Geel W, de Reus H, Biert J, Verbeek MM (2004) Glial and neuronal proteins in serum predict outcome after severe traumatic brain injury. Neurology 62:1303–1310.

Wang L, Zhou GB, Liu P, Song JH, Liang Y, Yan XJ, Xu F, Wang BS, Mao JH, Shen ZX, Chen SJ, Chen Z (2008) Dissection of mechanisms of Chinese medicinal formula Realgar-Indigo naturalis as an effective treatment for promyelocytic leukemia. Proc Natl Acad Sci USA 105:4826–4831.

Woertgen C, Rothoerl RD, Metz C, Brawanski A (1999) Comparison of clinical, radiologic, and serum marker as prognostic factors after severe head injury. J Trauma 47:1126–1130.

Xiong Y, Mahmood A, Chopp M (2009) Emerging treatments for traumatic brain injury. Expert Opin Emerg Drugs 14:67–84.

Young SH, Zhao Y, Koh A, Singh R, Chan BP, Chang HM, Venketasubramanian N, Chen C (2010) Safety profile of MLC601 (Neuroaid) in acute ischemic stroke patients: A Singaporean substudy of the Chinese medicine neuroaid efficacy on stroke recovery study. Cerebrovasc Dis 30:1–6.

(Accepted 19 June 2014)
(Available online 30 June 2014)

Neuroscience 278 (2014) 265–266

CORRIGENDUM

CORRIGENDUM TO ''MLC 901, A TRADITIONAL CHINESE MEDICINE INDUCES NEUROPROTECTIVE AND NEUROREGENERATIVE BENEFITS AFTER TRAUMATIC BRAIN INJURY IN RATS'' [NEUROSCIENCE 277 (2014) 72–86]

H. QUINTARD, [a,b] **T. LORIVEL,** [a] **C. GANDIN,** [a] **M. LAZDUNSKI** [a] **AND C. HEURTEAUX** [a]*

[a] *Institut de Pharmacologie Moléculaire et Cellulaire, Centre National de la Recherche Scientifique (CNRS), Université Nice Sophia Antipolis, 660 Route des Lucioles, 06560 Valbonne, France*

[b] *Centre Hospitalo-Universitaire de Nice, Hôpital St Roch, 4 rue Pierre Dévoluy, 06000 Nice, France*

The authors regret two mistakes:

(1) The composition of the MLC901 as presented on lines 7–12 of the ''Experimental design section'' on page 73 is in error. The correct composition of MLC901 per capsule was the following: 0.80 g Radix astragali, 0.16 g Radix salvia miltiorrhizae, 0.16 g Radix paeoniae rubra, 0.16 g Rhizoma chuanxiong, 0.16 g Radix angelicae sinensis, 0.16 g *Carthamus tinctorius*, 0.16 g *Prunus persica*, 0.16 g Radix polygalae, 0.16 g Rhizoma acori tatarinowii.
(2) The incorrect Fig. 7 was published. The correct Fig. 7 is presented here.

The authors would like to apologise for any inconvenience caused.

DOI of original article: http://dx.doi.org/10.1016/j.neuroscience.2014.06.047
*Corresponding author. Tel: +33-4-93-95-77-84; fax: +33-4-93-95-77-04.
E-mail address: heurteau@ipmc.cnrs.fr (C. Heurteaux).

http://dx.doi.org/10.1016/j.neuroscience.2014.08.004
0306-4522/

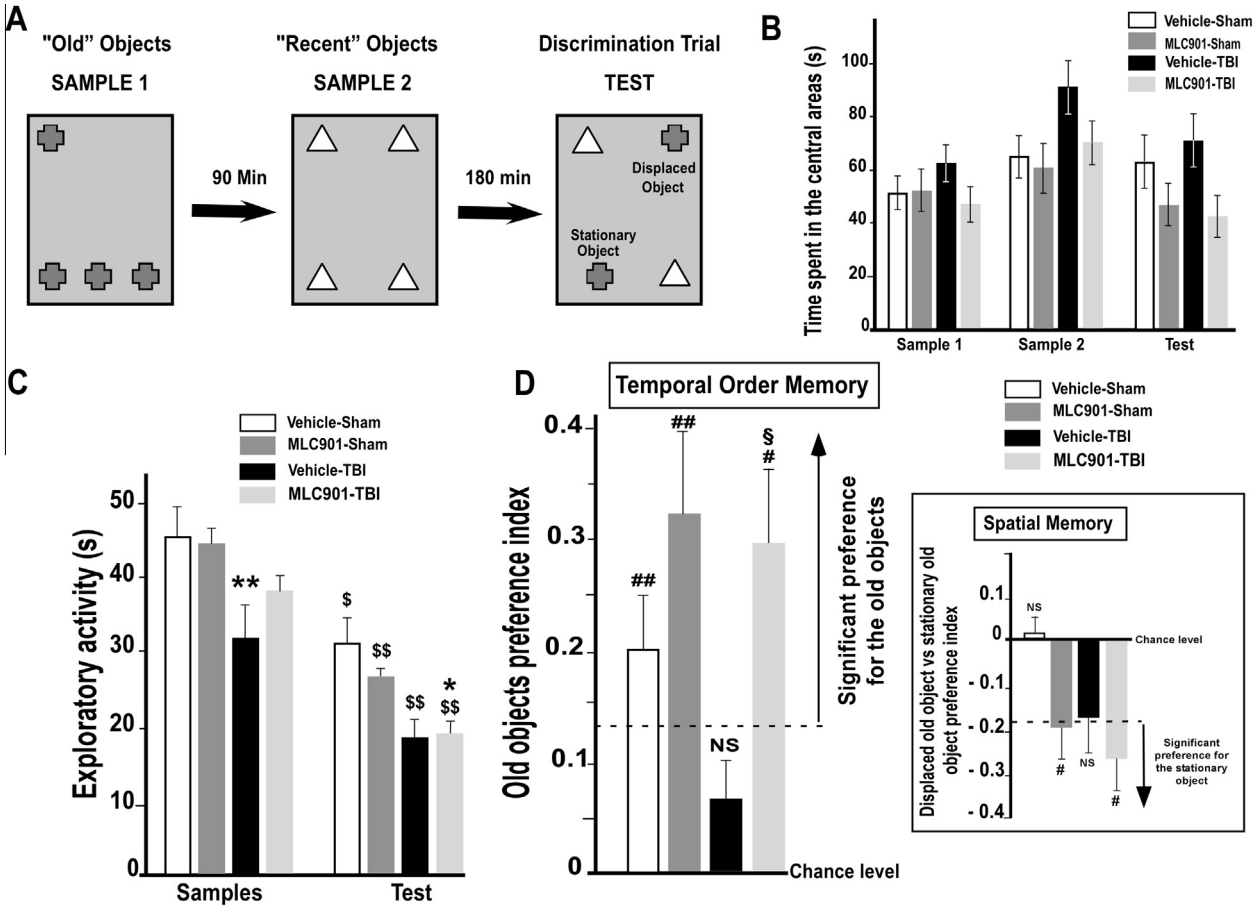

Fig. 7. MLC901 reverses TBI-related impairments of the episodic memory in the ''what, when, where'' task. The experimental groups were as follows: Vehicle-Sham, $n = 10$; MLC901-Sham, $n = 11$; Vehicle-TBI, $n = 10$; MLC901-TBI, $n = 9$. MLC901 (0.075 mg/ml, 500 microl/rat) was *i.p* injected 2-h post-TBI followed by an oral administration in drinking water (10 mg/ml) during 7 days. All values are mean ± SEM. (A) – Schematic drawing of the experimental design used. (B) – Anxiety level of animals. Neither the surgery nor MLC901 modified the anxiety-related behaviors of mice as detected by the time spent in the central area of the open field. All values are mean ± SEM. *Sample 1 trial*: Vehicle-Sham vs MLC901-Sham: $U = 52$; $P > 0.05$/Vehicle-TBI vs MLC901-TBI: $U = 25.5$; $P > 0.05$/Vehicle-Sham vs Vehicle-TBI: $U = 37.5$; $P > 0.05$/MLC901-Sham vs MLC901-TBI: $U = 41$; $P > 0.05$. (C) – Total exploratory activity. Only the first 6.5 min of each trial were considered. The samples exploratory time was obtained by averaging the *sample 1* and *sample 2* exploratory times. Comparison between Vehicle-Sham and Vehicle-TBI rats during the Samples trials: $U = 15$; $^{**}P < 0.01$. Comparison between Samples and Test exploratory times: Vehicle-Sham: $T = 8$; $^{\$}P < 0.05$/MLC901-Sham: $T = 0$; $^{\$\$}P < 0.01$/Vehicle-TBI: $T = 2$; $^{\$\$}P < 0.01$/MLC901-TBI: $T = 1$; $^{\$}P < 0.05$. (D) – Temporal order memory as denoted by preference index for the ''old'' objects during the first 6.5-min trial test. Comparison to chance level: Vehicle-Sham: $U = 55$; $^{\#\#}P < 0.01$/MLC901-Sham: $U = 65$; $^{\#\#}P < 0.01$/Vehicle-TBI: $U = 42.5$; $^{NS}P > 0.05$/MLC901-TBI: $U = 42$; $^{\#}P < 0.05$. Comparison between Vehicle-TBI and MLC901-TBI: $U = 18$; $^{\S}P < 0.05$. *Inset:* Object location (spatial) memory as denoted by the preference index for the ''stationary'' versus the ''displaced'' old object during the first 6.5-min trial test. Comparison to chance level: Vehicle-Sham: $U = 21$; $^{NS}P > 0.05$/Vehicle-TBI: $U = 45$; > 0.05/MLC901-Sham: $U = 48$; $^{\#}P < 0.05$/MLC901-TBI: $U = 42$; $^{\#}P < 0.05$.